



Demonstrating full-scale post-combustion CO₂ capture for coal-fired power plants through dynamic modelling and simulation

Adekola Lawal^a, Meihong Wang^{a,*}, Peter Stephenson^b, Okwose Obi^a

^a Process Systems Engineering Group, School of Engineering, Cranfield University, Beds MK43 0AL, UK

^b RWE npower, Windmill Hill Business Park, Swindon SN5 6PB, UK

ARTICLE INFO

Article history:

Received 29 September 2010

Accepted 26 October 2010

Available online 12 November 2010

Keywords:

Post-combustion CO₂ capture

Coal-fired power plant

Flexibility

Dynamic modelling and simulation

Scale-up

ABSTRACT

This study aims to provide insights into the design and operation of full-scale post-combustion CO₂ capture for a 500 MWe sub-critical power plant through dynamic modelling and simulation. The development and validation of the dynamic models of the power plant and CO₂ capture plant are described. In addition, the scale-up of the CO₂ capture plant from pilot plant scale (where it was validated) to full scale is discussed. Subsequently the manner in which the two plant models were linked is discussed. A floating IP/LP crossover pressure configuration is used. A throttling valve is included between the LP turbine and draw-off point to prevent pressures at the crossover from dropping below required levels in the reboiler for solvent regeneration. The flue gas from the power plant is treated before it is sent to the CO₂ capture plant. Four case studies are considered. The first investigates the effect of increasing solvent concentration on the performance of the power plant with the capture plant. The second investigates which absorber packing height offers a good balance between capital and operating costs. The two dynamic case studies show that the CO₂ capture plant has a slower response than the power plant. They also reveal an interaction of CO₂ capture level and power plant output control loops making it difficult to achieve steady power output levels quickly.

© 2010 Elsevier Ltd. All rights reserved.

1. Introduction

1.1. Background

Chemical absorption of CO₂ using MEA solvent has been recommended as a suitable technology for post-combustion power plants especially for retrofit purposes. Although the process technology has been applied in natural gas sweetening, the scale of process required to achieve up to 90% CO₂ capture in fossil fuel-fired power plants is typically several times larger than what is commercially available at present. For instance, Mitsubishi Heavy Industries (MHI) has built some of the largest plants that process up to 450 tonnes of CO₂ per day from natural gas fired boilers [1]. A 500 MWe supercritical coal-fired power plant operating at 46% efficiency (LHV basis) [2] would release over 8000 tonnes of CO₂ per day. To separate CO₂ from flue gas at that scale, a relatively large chemical absorption facility is required which would be a significant capital investment to the operator.

The operation of a power plant integrated with a chemical absorption process would present additional challenges. The efficiency of such plants would drop significantly because steam that

would have been used to generate electricity is drawn off to regenerate the solvent. Several studies have demonstrated that significant energy penalties would be incurred with the inclusion of carbon capture technology [3–5]. In addition, resultant reduced steam flows to the low pressure (LP) turbines would ultimately result in reduced pressures upstream of this point in the turbine. This and the possible process modifications required are described in the study. Another concern is whether such power plants could continue to play their role in meeting electricity demand. Coal-fired power plants currently operate flexibly in meeting varying electricity demand. Having power generation processes that could operate flexibly would be increasingly important with the growth of renewable power generation. Though renewable sources are virtually carbon neutral, they suffer the drawback of being intermittent in nature. Such variations in power generation increase the requirement for flexible operation in other plants on the same electricity grid. Hence, both the coal-fired power plant itself and the downstream CO₂ chemical absorption process would have to be capable of flexible operation.

1.2. Motivation

Design and operational studies are typically carried out with pilot and larger scale demonstration plants. Current pilot plant

* Corresponding author. Tel.: +44 1234 754655; fax: +44 1234 754685.

E-mail address: meihong.wang@cranfield.ac.uk (M. Wang).

Nomenclature

A	cross-sectional area (m^2)	σ	Stefan–Boltzmann constant
f	fugacity coefficient	μ	viscosity (Pa s)
F_i	component mass flow rate (kg/s)	ω	wetted area ratio
F_H	Enthalpy flow rate (J/s)	χ	diffusivity (m^2/s)
F_{LV}	flow parameter	γ	CO_2 loading (mol CO_2 /mol MEA)
g	acceleration due to gravity (m^2/s)	Subscripts	
G	gas flowrate (m^3/s)	<i>abs</i>	absorption
H	heat flux (J/m^2)	<i>ad</i>	adiabatic
h	specific enthalpy (J/kg)	<i>ave</i>	average
HL	heat loss to surroundings (J/m^3)	<i>DC</i>	downcomer
K	empirical constant	<i>DCB</i>	downcomer bottom
K_4	pressure drop parameter	<i>eff</i>	effective
L	height of column section (m)	<i>evap</i>	evaporative
L/G	liquid to gas mass flow rate	<i>FW</i>	feed water
LHV	lower heating value	<i>g</i>	gas
M	mass holdup (kg/m^3)	<i>H</i>	enthalpy
m	mass flowrate (kg/s)	<i>i</i>	component number
MW	molecular weight (kg/mol)	<i>Liq</i>	liquid
N	molar flux ($\text{mol}/\text{m}^2\cdot\text{s}$)	<i>MR</i>	riser tube metal
NAE	number of axial elements	<i>R</i>	riser
nc	number of components	<i>s</i>	steam
P	pressure (Pa)	<i>TD</i>	total (drum)
Q	heat flow (J/s)	<i>tfr</i>	thrown-forward radiation
Q_{NCV}	net calorific value (J/kg)	<i>WDC</i>	water in downcomer
R	universal gas constant (J/mol K)	<i>WR</i>	water in riser
Sp	specific area (m^2/m^3)	<i>WRO</i>	water out of riser
T	temperature (K)	<i>Vap</i>	vapour
U	energy holdup (J/m^3)	Superscripts	
V	volume (m^3)	<i>Cond</i>	conduction
V	gas mass flowrate per unit cross-sectional area ($\text{kg}/\text{m}^2\text{ s}$)	<i>Conv</i>	convection
X	mass fraction	<i>I</i>	interface
x_i^M	molar fraction	<i>L</i>	liquid
y	axial position	<i>Lb</i>	liquid bulk
z	film position	<i>Lf</i>	liquid film
Greek symbols		<i>M</i>	molar
β	constant for estimating effective gas temperature	<i>R</i>	reference
δ	film thickness (m)	<i>V</i>	vapour
λ	thermal conductivity (W/m K)	<i>Vb</i>	vapour bulk
ρ	density (kg/m^3)	<i>Vf</i>	vapour film

studies worldwide are on a much smaller scale than would be required commercially. Even at such scales (typically less than 5 MWe), the cost of construction for these facilities typically runs up to several million dollars [6]. Once built, these plants are limited in the range of studies that could be carried out. Full scale demonstration projects are estimated to cost over a billion dollars [6]. A lot of useful insights could be derived from accurate dynamic models of the post-combustion capture process at a much lower cost.

Most process models developed to study cost and performance implications of carbon capture and storage (CCS) have been steady state models which cannot account for the various transients associated in the power generation process. Transients occur during plant start-up and shutdown operations. Load-following operations are common in coal-fired power plants. Operational problems could be further compounded if there are tight restrictions on CO_2 emissions. The downstream absorption plant may have to closely follow load changes. Finally, to improve overall efficiency, increased process integration of the power generation process and capture process would be required. This would likely further complicate the operation of the integrated facility. Insights regarding

the integrated plant operation could also be provided through studies using dynamic modelling and simulation.

1.3. Previous research

A number of studies have been carried out on dynamic model development of the chemical absorption plant. Kvamsdal et al. [7] and Lawal et al. [8] present the dynamic model development and simulation of the absorber only. Lawal et al. [8] also discusses different types of models used for modelling reactive absorption and the developments made in this regard. Rate-based models are shown to be more accurate than equilibrium-based ones. Ziaii et al. [9] describes the dynamic model development and simulation of the regenerator only while Lawal et al. [10] extends this to the two stand-alone absorber and regenerator column models. Analysis on stand-alone columns may be inaccurate due to the inevitable coupling of the two columns linked with a recycle loop. Lawal et al. [11] describes the dynamic model development of the chemical absorption process (absorber and regenerator linked by recycling the solvent). This model, however, was developed and validated

at pilot plant scale, three orders of magnitude smaller than what is required for processing flue gas from a coal-fired power plant generating 500 MWe. Lawal et al. [12] investigated the performance and dynamic response of the chemical absorption process downstream an enhanced oxygen coal power plant and demonstrated how there was room for further improvement of performance by addressing the increased absorber temperatures.

A number of studies explored the dynamic response of power plants. Lu [13] combined a dynamic model with steady state correlations to simulate power plant component dynamics in MATLAB/SIMULINK. The components could be linked to form a power plant. The dynamic model developed was not validated though some simulation results for a whole plant were shown. Åström and Bell [14] derived a model from first principles to describe the drum, downcomer, and riser components of a natural circulation drum-boiler. Bhambare et al. [15] modelled from first principles a 250 MW coal-fired natural circulation boiler. The boiler system was divided into seven submodels: downcomer, riser, waterwall, drum, superheater and reheater, attemperator, and furnace. Chaibakhsh et al. [16] developed a dynamic model of a sub-critical once-through Benson type boiler based on the experimental data obtained from a complete set of field experiments. Genetic algorithm (GA) was executed to estimate the model parameters and fit the models response on the real system dynamics. Stephenson et al. [17] developed dynamic models of a sub-critical coal-fired power plant in gPROMS and validated the results with plant data. Power plant models described by these authors do not include integration with a CO₂ capture plant.

Steady state models of the CO₂ capture plant integrated with the power plant have been developed. A steady state, in-house model was used by Aroonwilas and Veawab [18] to compare the performance of different process configurations and different solvents (including solvent blends) for the chemical absorption plant integrated with a supercritical power plant. Sanpasertparnich et al. [19] carried out a study of the integration of the two plants using a steady state model. The model also considered CO₂ compression. Another steady state integration study was carried out by Cifre et al. [20]. In this study, the impact of CO₂ compression was considered as well and efficiency penalties estimated were up to 16%.

1.4. Scope of the study and novelties of the paper

This study was conducted with a modelling and simulation approach. The gPROMS (Process Systems Enterprise Ltd.) advanced process modelling environment has been used to implement the proposed work. Dynamic models of the CO₂ chemical absorption plant and a 500 MWe sub-critical coal-fired power plant were developed. A sub-critical plant was used rather than a supercritical one because there was plant data available for dynamic validation obtained from one of the plants RWE npower operates. The two dynamic process models were linked together to carry out a unique study of their integrated operation.

2. CO₂ capture plant model development and validation

Rate-based dynamic models of the CO₂ absorption process consist mainly of the absorber and regenerator column model. Mass transfer rates in the columns were modelled based on the two-film theory using the Maxwell–Stefan formulation while the reactions were assumed to attain equilibrium. Dynamic validation of the CO₂ absorption model was carried out at pilot plant scale. The model was subsequently scaled up to full scale and therefore able to process the flue gas from a 500 MWe sub-critical power plant.

2.1. Model assumptions

The following assumptions were used in developing this dynamic model:

- (a) All reactions are assumed to attain equilibrium.
- (b) Plug flow regime and linear pressure drop along the column.
- (c) Phase equilibrium at interface between liquid and vapour films.
- (d) Negligible holdup in the vapour bulk.
- (e) Negligible solvent degradation.
- (f) Negligible heat loss in the absorber column.

2.2. Model equations

The amine plant consists of two main packed columns – the absorber and regenerator. More details of the absorber and regenerator dynamic model are described in [11]. In the packed column section, the main models include the vapour and liquid bulk models, the vapour and liquid film models and the interface (Fig. 1).

The main equations are listed for the convenience of readers.

For the liquid bulk, the mass and energy balance equations are listed.

$$\text{Mass Balance : } \frac{dM_i}{dt} = \frac{-1}{L \cdot A} \frac{\partial F_i^L}{\partial y} + N_i \cdot Sp \cdot MW_i \cdot \omega \quad (1)$$

$$\text{Energy Balance : } \frac{dU}{dt} = \frac{-1}{L \cdot A} \frac{\partial F_H^L}{\partial y} + Sp \cdot \omega \cdot (H_{liq}^{cond} + H_{liq}^{conv} + H_{abs}) + HL \quad (2)$$

The change in component mass holdup, M_i , with respect to time is determined by the differential change of the component mass flow along the axis of the column $\frac{\partial F_i^L}{\partial y}$ and the estimated component molar fluxes to and from the liquid bulk N_i . Molar fluxes are determined using the Maxwell–Stefan formulation in the liquid and vapour film models.

The change in energy holdup with respect to time, $\frac{dU}{dt}$, is determined by the differential change of ‘energy flow’ along the axis of the column, $\frac{\partial F_H^L}{\partial y}$ and the liquid heat fluxes at the liquid film–liquid bulk interface due to conduction, H_{liq}^{cond} , convection, H_{liq}^{conv} as well as the heat flux due to chemical absorption of CO₂, H_{abs} . Heat fluxes due to conduction and convection are accounted for in the film models.

$$\text{Heat Loss (HL)} = \frac{131.64 \times \text{Column Surface Area} \times (T_{\text{regen_bottom}} - T_{\text{ambient}})}{\text{Height} \times \text{Cross Sectional Area} \times \text{NAE}} \quad (3)$$

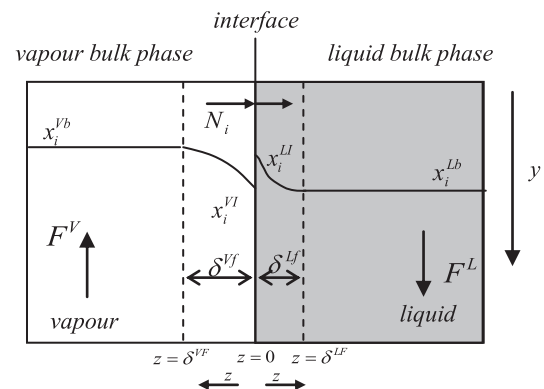


Fig. 1. Liquid and vapour bulks, films and interface.

The Heat Loss (HL) in the regenerator is calculated based on the temperature difference between the regenerator bottoms temperature ($T_{\text{regen_bottom}}$) and the ambient temperature (T_{ambient}). It is calculated per unit volume and distributed evenly along the axial length of the column by dividing by the Number of Axial Elements modelled in the column section (NAE). The constant value was derived from a correlation from the University of Texas at Austin test results [21].

$$\text{Heat of absorption(or desorption)} : H_{\text{abs}} = N_{\text{CO}_2} \cdot h_{\text{abs}} \quad (4)$$

$$h_{\text{abs}} = R \cdot \left(-14281 - \left(\frac{1092554 \cdot \gamma^2}{T} \right) - \left(\frac{6800882 \cdot \gamma}{T} \right) + 32670.01 \cdot \gamma \right) \quad (5)$$

The specific heat of absorption, h_{abs} , was estimated based on the temperature, T , and the CO_2 loading of the solvent, γ . R is the universal gas constant [22].

The vapour bulk model has a similar structure to that of the liquid bulk model with the exception of the mass and energy accumulation terms which are assumed to be negligible in the vapour phase. At the interface between the liquid and vapour films, phase equilibrium is assumed to exist such that:

$$f_i^L \cdot x_i^{M,L} = f_i^V \cdot x_i^{M,V} \quad (6)$$

Phase equilibrium between liquid and vapour phases is assumed at the interface. The equilibrium molar compositions of the components in the vapour and liquid phases, x_i^M , are estimated based on the vapour and liquid fugacity coefficients, f_i .

2.3. Controllers for the process

Control schemes are illustrated in Fig. 9. More details are presented in [11].

2.4. Model validation at pilot plant scale

The steady-state validation of the chemical absorption plant model was carried out using data from one of the cases of the Separations Research Program at the University of Texas at Austin [21]. The absorber and regenerator columns of the pilot plant were both packed columns with diameters of 0.427 m and total packing height of 6.1 m. It is shown that the models give good predictions of the shape of the temperature profiles for both absorber and regenerator (referred to as the rate-based stand-alone model) [8]. Further validation studies have been carried out for the amine plant set-up (where the absorber and regenerator columns have been linked with recycle referred to as the rate-based integrated

model) [10,11]. Validation results are shown for the absorber and regenerator in Fig. 2.

The steady state predictions of the integrated model were found to be slightly better than the stand-alone models. In the latter, estimates of the input to the column had to be made and errors in such guesses would affect overall results. This suggests that the model predicts the interaction between the component parts of the plant (mainly the two columns) fairly well. It should be noted that the pilot plant in the study used to validate these results did not have a cross heat exchanger but used a combination of a heater and cooler [11,21]. Dynamic validation of the model could not be carried out because of the unavailability of dynamic plant test data.

2.5. Scale-up for absorber and stripper

Based on the experience gained from pilot plant studies and Chemical Engineering principles, the sizes, heat duties, configurations etc. of the unit operations required to process the flue gas from a 500 MWe sub-critical power plant were determined. This design would also suffice for a 600 MWe supercritical power plant which would have similar flue gas flows and composition. The system was designed to capture 90% of the CO_2 from 600 kg/s of flue gas from the power plant using a 30 wt.% MEA solution. Preliminary design calculations were carried out with the following assumptions, providing the “Initial guess”. The following assumptions were used:

- Similar operating pressures for the absorber and regenerator used in the pilot plant study were used at full scale (1 bar and 1.6 bar respectively).
- MEA solvent absorption capacity was assumed to be 0.18 mol CO_2 / mol MEA which was used to calculate the solvent circulation rate.
- All SO_2 and NO_x have been removed from the flue gas stream.
- There is no water wash section in the absorber.
- Water balance is achieved using a water makeup control system.

To process increased volumes of flue gas, the column diameters must be correspondingly increased. The approach used to determine the required column diameters of the absorber and the regenerator is described in Sections 2.5.1 and 2.5.2, respectively.

2.5.1. Number of absorber columns and absorber diameter based on the generalized pressure drop correlation

Due to the structural limitations, [23] suggests that column diameters should not exceed 12.2 m (40 feet). To process the large

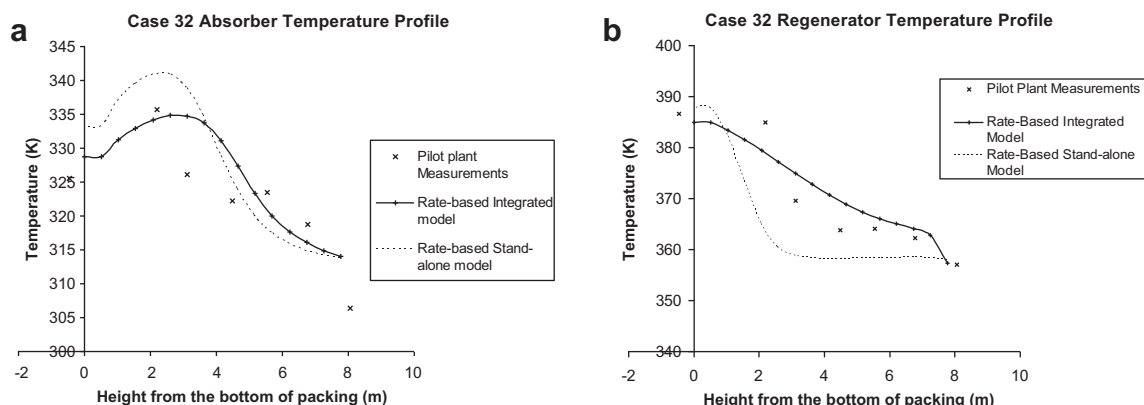


Fig. 2. (a) Absorber and (b) regenerator temperature profile of columns for case 32.

volumes of flue gas from the power plant, more than one absorber column may be required. In addition, using more than one absorber column could help improve the turndown ratio of the process. Coal-fired power plants traditionally operate flexibly to meet varying demand. If such plants are fitted with post-combustion capture, it would be of advantage if they could continue to play such a role. The CO₂ capture process may therefore need to be designed

to accommodate a large turndown ratio which would be easier to achieve with more than one column.

On the other hand, [3] reports that the absorber would most likely be the largest equipment in the capture plant since it would process huge volumes of flue gas. To provide a balance, therefore, the minimum number of columns required should be selected to keep capital costs down and minimize footprint requirements. The capacity of the absorber is largely based on its cross-sectional area. The column is usually designed to operate at the highest economical pressure drop to ensure good liquid and gas distribution [24].

The operating region of the packed column is limited by two main mechanisms: flooding and minimum liquid load [25]. Flooding sets the upper capacity of limit of the packed column. At this point, the pressure drop of the gas flow increases to an extent that the liquid is no longer able to flow downward against the gas flow [25]. The minimum liquid load refers to ensure lowest liquid flow rate sufficient mass transfer. Beyond this point, only a small proportion of the packing surface is wetted [25]. Fig. 3 illustrates these limits.

The required solvent flow rate (liquid load) was estimated based on the estimates specified in Table 1.

Sinnott [24] gives the recommended pressure drop per metre packing for absorbers and strippers as 15 to 50 mm of water per metre of packing height typically away from the flooding line (Fig. 4). Forty-two mm of water per metre of packing height was used for the design of both the absorber and stripper columns based on the recommendation of operating at the highest economical pressure drop [24].

F_{LV} is a flow parameter dependent on the L/G ratio of the column while K_4 is a modified gas load [25]. Based on the estimated F_{LV} flow parameter and the pressure drop parameter value chosen, the K_4 value is obtained from Fig. 4.

$$K_4 = \frac{13.1 (V_w^*)^2 \cdot F_p \cdot \left(\frac{\rho_L}{\rho_v}\right)^{0.1}}{\rho_v \cdot (\rho_L - \rho_v)} \quad (7)$$

Table 1
Calculation of required lean solvent flow.

Description	Value
Flue gas mass flow rate (kg/s)	600
Flue gas mass composition (N ₂)	0.748
Flue gas mass composition (CO ₂)	0.209
Flue gas mass composition (H ₂ O)	0.042
Lean solvent mass fraction (MEA)	0.3048
Lean solvent mass fraction (CO ₂)	0.0618
Lean solvent mass fraction (H ₂ O)	0.6334
Estimated required lean solvent mass flow (kg/s)	2900

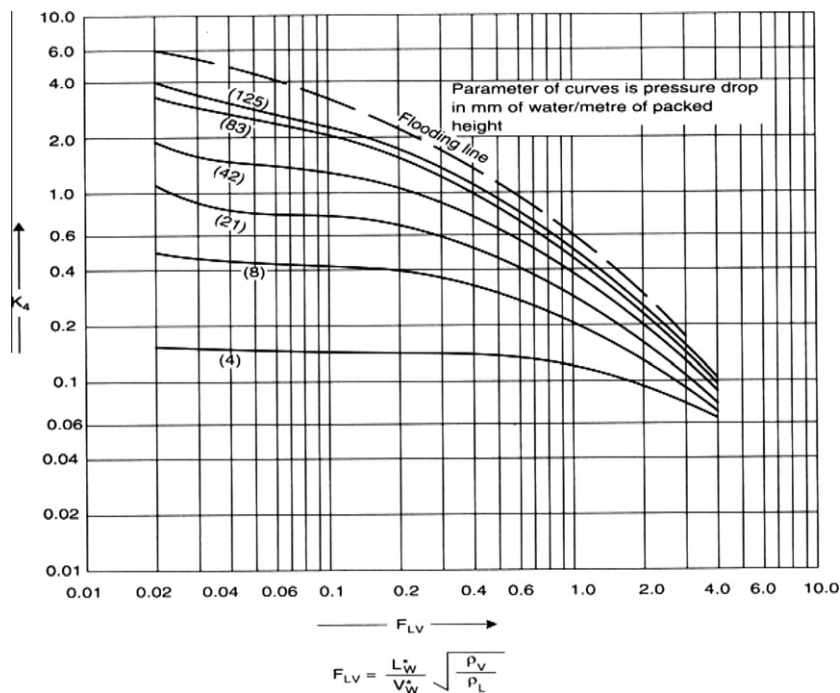


Fig. 4. Generalized pressure drop correlation from [24].

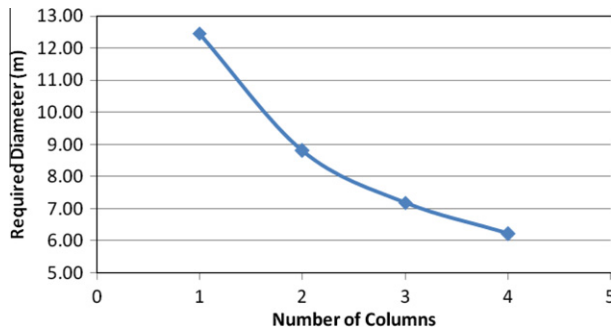


Fig. 5. Required absorber diameter based on the number of absorber columns.

Table 2

Summary of preliminary design parameters for chemical absorption plant.

Description	Value
Design flue gas mass flow rate (kg/s)	600
CO ₂ mass fraction in flue gas	0.21
CO ₂ capture level (%)	90
Absorber column number	2
Absorber diameter (m)	9
Absorber height (m)	17
Regenerator column number	1
Regenerator column diameter (m)	9
Absorber operating pressure (10 ⁵ Pa)	1.01
Regenerator operating pressure (10 ⁵ Pa)	1.62
Lean solvent mass fraction (MEA)	0.3048
Lean solvent CO ₂ loading (mol CO ₂ /mol MEA)	0.29

μ_l = liquid viscosity

F_p = packing factor (dependent on the packing size and type)

The V_w^* term stands for the vapour mass flow rate per unit cross-sectional area. It is estimated from Eq. (7) and is then used to estimate the required cross-sectional area of the column and thus the diameter. The estimated absorber diameters required for 1–4 absorber columns in parallel are displayed in Fig. 5.

From Fig. 5, one absorber column would require a diameter of over 12 m which would exceed 40 feet. In addition, the turndown ratio of such a column may be significantly limited. Two or three columns could be selected with diameters of 9 m and 7 m, respectively. For this study, a two-column absorber configuration was selected to minimize the footprint required for the columns. Selecting three or four columns may not provide significant returns in comparison with the large capital cost and footprint requirements this would demand.

2.5.2. Regenerator diameter

Earlier simulation studies have shown that the regenerator processes much less volumetric vapour flow than the absorber; thus, a single column could be used. From the generalized pressure drop correlation method used above, the regenerator diameter was estimated as 8.39 m, thus a single 9 m diameter column would suffice.

It was impossible to validate the chemical absorption plant model at 500 MWe scale because no plant existed at the time of this study. The summary of the specifications for the two columns in the CO₂ capture plant are shown in Table 2.

3. Sub-critical coal-fired power plant model development and validation

Dynamic models for the furnace, boiler, 3-stage steam turbine, condenser and feed-water system were developed. The model was dynamically validated using plant data.

3.1. Model development

The block flow diagram of the power plant model is shown in Fig. 6.

3.1.1. Furnace model

Pulverized fuel (coal) is supplied to the furnace with the aid of primary air. The coal specification is given in Table 3. The furnace model includes only the air/gas side and as such it was assumed to be steady state since variables would adjust very quickly to any

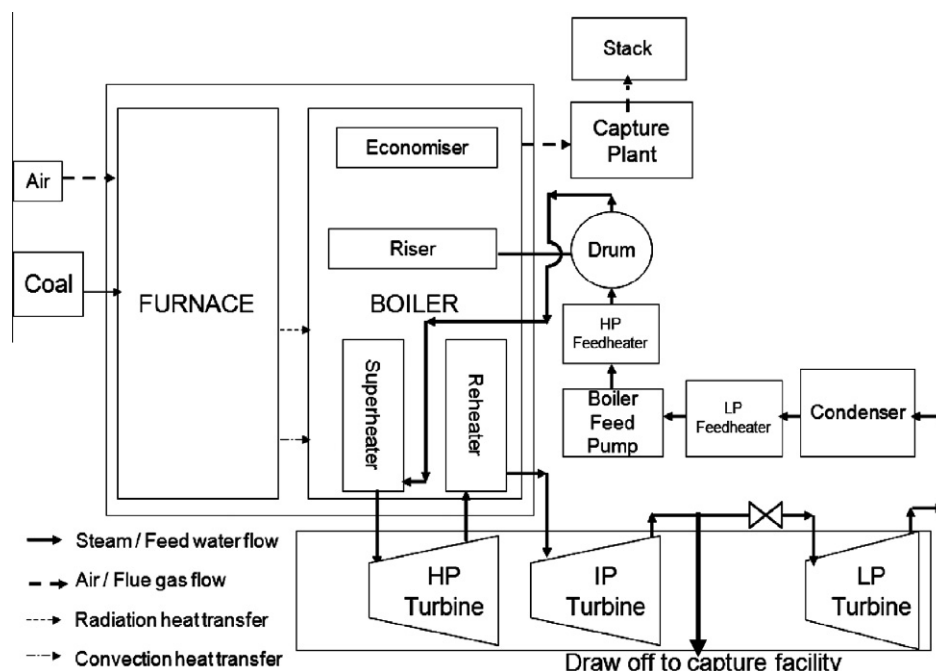


Fig. 6. Power plant model block flow diagram.

Table 3
Coal specification for power plant model.

Composition % mass, as received basis	
Moisture	8
Ash	20
C	59.11
H	3.99
N	1
S	2.0
O	5.9
CV, MJ/kg, as received basis	
GCV	24.51
NCV	23.33

changes in inlet or boundary conditions. The overall heat balance is given in Eq. (8).

$$h_{in}m_{air,in} + h_{fuel}m_{fuel} + Q_{NCV}m_{fuel} = h_{out}m_{g,out} + h_{ash}m_{ash} + Q_{evap} + Q_{tfr} \quad (8)$$

The heat generated in the furnace by the combustion of pulverized fuel supplied at the fuel mass flow rate (fuel burn rate), m_{fuel} , is estimated based on the coal Net Calorific Value, Q_{NCV} . The heat generated in addition to the total enthalpy of the combustion air ($h_{in}m_{air,in}$) and fuel ($h_{fuel}m_{fuel}$) determine the total enthalpy of the outlet streams (flue gas and ash) as well as the heat transferred to the evaporative circuit, Q_{evap} and the thrown-forward radiation, Q_{tfr} . The air and gas enthalpies (h_{in} and h_{out}) are obtained from Multiflash physical property package that uses Lee–Kesler–Plöcker equation of state. To calculate Q_{evap} and Q_{tfr} it is necessary to calculate the adiabatic flame temperature. This is done from a heat balance equation similar to that given earlier, but with the outlet temperatures and enthalpies equal to the adiabatic flame temperature and with Q_{evap} and Q_{tfr} both equal to zero. An effective gas temperature is then found from the adiabatic and outlet temperatures:

$$T_{eff} = \beta T_{g,ad} + (1 - \beta)T_{out} \quad (9)$$

Here, $T_{g,ad}$ is the adiabatic flame temperature and β is a user-input constant.

Then the evaporative heat is found based on κ_{evap} , a user-input constant; V_{furn} , the furnace volume; σ , the Stefan–Boltzman constant and $\rho_{g,out}$, the gas density at furnace outlet as shown in Eq. (10).

$$Q_{evap} = \frac{\kappa_{evap} V_{furn} \sigma (T_{eff})^4}{\rho_{g,out}} \quad (10)$$

The thrown-forward radiation, Q_{tfr} , is found from a similar equation; the only difference is the use of a different constant, κ_{tfr} .

3.1.2. Downcomer, riser and drum models

Heat generated in the furnace is transferred to the water walls (downcomer and risers), superheaters, reheaters and economisers. The mass flow rate of water in downcomer, \dot{m}_{WDC} was modelled as proportional to the pressure drop in the downcomer [26].

$$\dot{m}_{WDC} = K_{DC} \sqrt{(P + \rho_{WDC} g Z - P_{DCB}) \rho_{WDC}} \quad (11)$$

K_{DC} is an empirical constant that relates the pressure drop (estimated from the top (P) pressure, the hydrostatic pressure exerted by the water in the downcomer ($\rho_{WDC} g Z$) and the bottom downcomer pressure, P_{DCB}) and water density in downcomer, ρ_{WDC} to the mass flow rate.

Heat transfer is modelled in the riser section. The mass balance of fluid in the riser is given as [26]:

$$\dot{m}_{WDC} = \dot{m}_{WRO} = V_R \frac{d\rho_{WR}}{dt} \quad (12)$$

Enthalpy balance for water/steam in riser [26]:

$$V_R \frac{dh_{WR}}{dt} = Q_{WR} + \dot{m}_{WRO}(h_{WDC} - h_{WR}) \quad (13)$$

The heat transferred to the water in the riser tubes, Q_{WR} is given as

$$Q_{WR} = K_{WR} \cdot (T_{MR} - T_{WR})^3 \quad (14)$$

K_{WR} is an empirical constant that estimates the heat transfer based on the cube of the temperature difference between the riser tube walls (T_{MR}) and the steam temperature at the riser exit (T_{WR}). \dot{m}_{WRO} , the mass flow of water at riser exit is estimated in a similar manner to the \dot{m}_{WDC} in Eq. (11).

The fluid at the riser exit is a mixture of vapour and liquid phases. The fraction of liquid in the mixture entering the drum, XR is estimated based on the exit specific enthalpy (h_{WR}) and density (ρ_{WR}) based on the liquid and vapour specific enthalpies and densities.

Dynamic mass balance for steam in drum is [26]:

$$\dot{m}_{WRO} \cdot XR - \dot{m}_{DO}^V = (V_{TD} - V_{WD}) \frac{d\rho_D^V}{dt} \quad (15)$$

This equation determines the mass flow of steam out of the drum, \dot{m}_{DO}^V . It is assumed that there is no heat loss from the drum to the surroundings.

Mass balance for water in drum is [26]:

$$\frac{dM_{WD}}{dt} = \dot{m}_{FW} + \dot{m}_{WRO}(1 - XR) - \dot{m}_{WDC} \quad (16)$$

\dot{m}_{FW} is the mass flow of feed water into drum.

3.1.3. Heat exchanger-type models (superheater and reheater)

A transient heat exchanger model was used to model convective heat transfer in the superheater and reheater. The superheater platens and secondary superheater also accounted for radiative heat transfer. The model accounts for changes on the steam side as well as the gas side.

Mass balance for steam side

$$\dot{m}_{s,out} = \dot{m}_{s,in} - V_s \frac{d\rho_s}{dt} \quad (17)$$

Here, $\dot{m}_{s,out}$ and $\dot{m}_{s,in}$ are the mass flow rates of steam in and out of the tube. ρ_s is the steam density. V_s is the volume of steam in the tube.

Enthalpy balance for steam side (h_s)

$$\rho_s V_s \frac{dh_{s,out}}{dt} = m_{s,in} h_{s,in} - m_{s,out} h_{s,out} + U_s (T_w - T_{s,ave}) \quad (18)$$

Here, the overall admittance factor U_s is a function of the overall heat transfer coefficient. $T_{s,ave}$ is the average steam temperature.

Radiative heat transfer, q_{rad} is estimated based on the Stefan–Boltzmann law.

$$q_{rad} = \frac{k_{wall} V_g \cdot \sigma \cdot T^4}{\rho_g} \quad (19)$$

3.2. Important control systems

Superheater temperatures are controlled using spray water atomizers. These essentially mix the steam with controlled flows of spray water to achieve required temperatures. Reheater

temperatures are controlled by using rear gas pass biasing dampers which control the flow of flue gas along the divided rear pass. The fuel burn rate and governor valve both control power plant power output. The target power plant output is directly controlled by the governor valve; this target also sets the target drum pressure. The drum pressure is controlled by the fuel burn rate.

3.3. Turbine models

These models apply generally to the High, Intermediate and Low Pressure turbines. The Overall pressure ratio, r governing their operation is given:

$$r = P_{out}/P_{in} \quad (20)$$

3.4. Model validation of power plant model

The power plant model developed in gPROMS was validated on a steady state and dynamic basis. The steady state model results were compared with the plant design data shows satisfactory agreement. Details of the validation are discussed in [17]. It should be noted that recent plant data from Didcot suggests lower thermal efficiency compared with design values [17].

The model was also validated dynamically against plant data. The plant data chosen for validation was as follows:

1. Frequency-following operation at nominally 417 MWe gross, 146 bar drum pressure.
2. Transient with the gross MWe rising linearly to nominally 469 MWe gross, 163 bar drum pressure corresponding to an increase of 52 MWe in 32 min, i.e. 0.3% of full load per minute.
3. Frequency-following operation at nominally 469 MWe gross, 163 bars drum pressure.

A comparison between plant data and power plant model predictions for the transients is given in [17] showing that the gPROMS model predicted flows fairly well through the course of the test.

4. Linking the power plant model with the CO₂ capture model

Three main links are included between the power plant and the CO₂ capture plant, as follows.

- a. The flue gas stream which is to be processed.
- b. The steam draw-off from the power plant to the capture plant to regenerate solvent in the reboiler.
- c. The condensate return from the reboiler to the power plant.

The linked model for power plant and CO₂ capture plant is subsequently referred to as the whole plant model.

4.1. Flue gas pre-processing

Flue gas from the power plant must be cooled down to between 40–50 °C for best absorption performance in the absorber. Gases like sulphur oxides and nitrous oxides form heat stable salts with MEA solvent (which cannot be regenerated). SO₂ concentrations of less than 10 ppm are recommended. SO₂ removal is usually achieved in a Flue Gas Desulphurization (FGD) unit. NO_x is removed using Selective Catalytic Reduction (SCR), Selective Noncatalytic Reduction (SCNR) or low NO_x burners. Particulates in the flue gas could clog the column packings and increase problems due to foaming. Particulate matter such as fly ash is removed by either electrostatic precipitators or bag house filters.

In the whole plant model, it is assumed that all the SO₂ and NO_x is removed upstream of the absorber and a Direct Contact Cooler (DCC) reduces the flue gas temperature to 40 °C. All the particulate matter is assumed removed. In addition, the effect of oxygen in the degradation of MEA solvent is neglected. Thus oxygen is considered inert and its composition is simply incorporated in the nitrogen composition (Fig. 7).

A blower adds the required head necessary to feed the flue gas to the absorber at just above atmospheric pressure. A splitter splits the flue gas flow into two equal streams that feed the two identical absorber columns as shown in Fig. 7.

4.2. Steam draw-off

Steam is drawn off at the IP/LP crossover as recommended by Ramezan and Skone [23] and Lucquiaud and Gibbins [27] amongst other authors. Due to the reduced flow through the turbine, the pressure upstream the LP turbine drops. The steam draw-off setup is shown in Fig. 8. This drop in pressure could be estimated by Stodola's Ellipse law [28]. The floating IP/LP crossover pressure configuration was employed [19,27]. This would accommodate a variable flow rate of steam draw-off. A throttling valve between the steam draw-off point and the LP turbine adds an additional pressure drop to raise the crossover pressure by about 1 bar. This ensures that the pressure across the IP/LP crossover does not drop below the required pressure needed in the reboiler (at least 3 bar). To employ this configuration, it is assumed that the IP turbine can accommodate the reduced exit pressures encountered with the steam draw-off [27].

A temperature controller measures the temperature of the lean solvent stream from the reboiler and controls the amount of steam drawn-off for regeneration using a control valve as shown in Fig. 8. A water spray is used to cool down the steam temperature to just above saturation. It is assumed that there is no loss of total enthalpy in the process as the additional sensible heat was converted to latent heat of the vaporized spray water. This stream is then supplied to the reboiler where it exchanges heat with the solvent. It is assumed that all steam supplied condenses in the reboiler leaving saturated liquid condensate at the outlet. It is also assumed

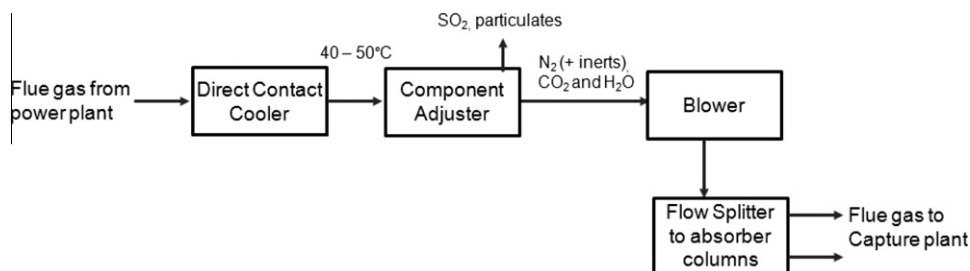


Fig. 7. Linking the flue gas from the power plant with the CO₂ capture plant model.

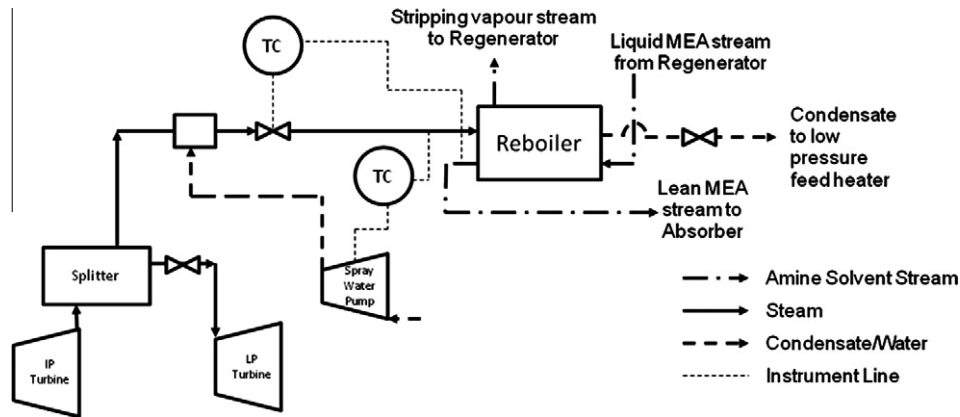


Fig. 8. Steam draw-off and condensate return.

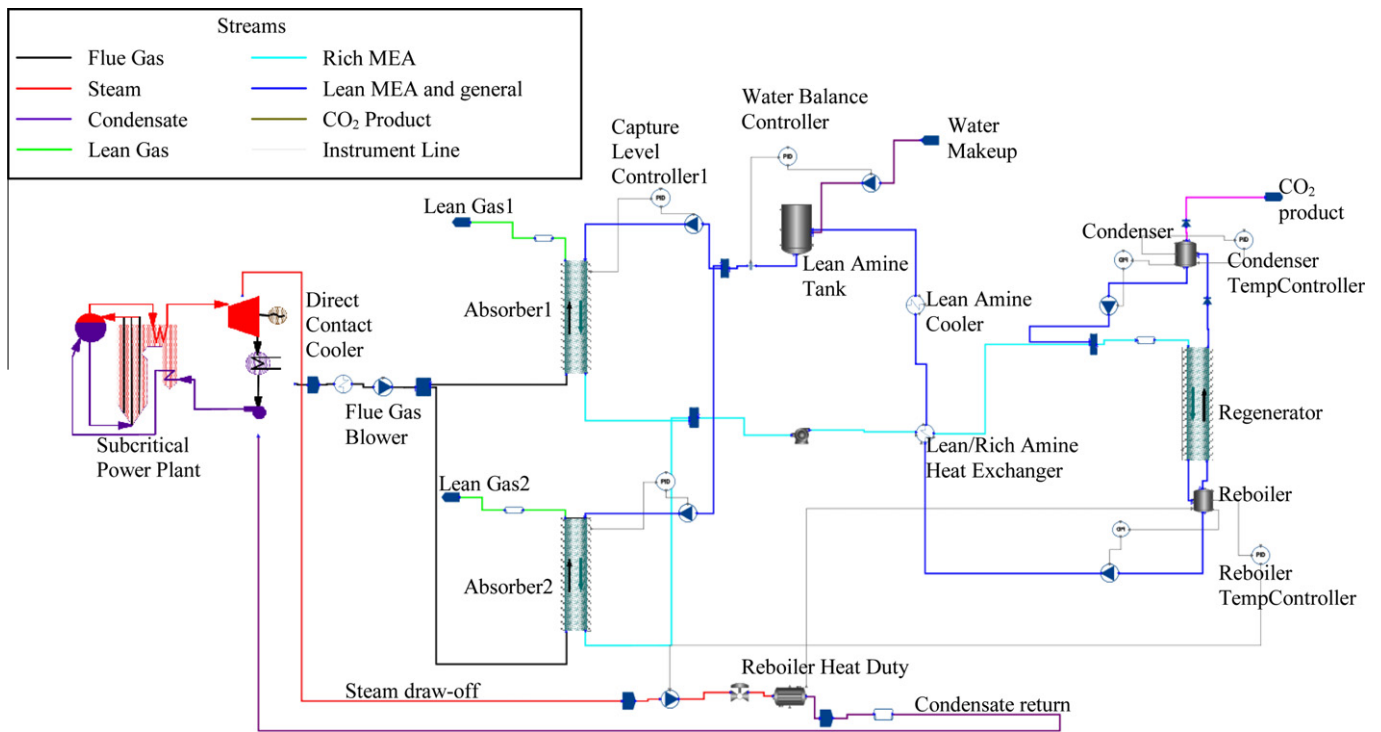


Fig. 9. Whole Plant Model Topology.

that there are no heat losses and all the latent heat of vaporization is transferred to the reboiler fluid.

4.3. Condensate return

The condensate returned to the low pressure feedheater before being sent to the boiler feed pump. These two links between the power plant and CO₂ capture plant are shown in Fig. 8.

4.4. Whole plant model topology

The whole plant model topology is shown in Fig. 9.

5. Case studies

Two steady state and two dynamic case studies are presented based on simulation results from the whole plant model described in Section 4:

Steady state cases

- Plant performance with different absorber heights.
- Plant performance with and without CO₂ capture and at different concentrations of MEA.

Dynamic cases

- Reducing power plant output.
- Increasing capture level set point from 90% to 95%.

5.1. Case study 1 – increasing absorber packing height

Different packing heights of each of the absorber columns were tested to study the effect of increasing absorber packing height on the performance of the system. The parameter used to determine the effectiveness of each case was the heat requirement for CO₂ capture – the amount of heat required to separate 1 kg of CO₂ from

the flue gas mixture. The same design parameters summarized in Table 2 were used and absorber packing heights ranging from 17 to 37 m were tested. Cifre et al. [20] estimated that the absorber column design should be performed with a minimum height of 17 m for the random IMTP50 packing considered. For each case, the capture level controller was set to capture 90% of the CO₂ in the flue gas. The results are presented in Fig. 10. It is shown that significant savings of about 0.7 MJ/kg CO₂ could be achieved whilst increasing absorber packing heights from 17 to 25 m. There appears to be diminishing returns in the reduction in heat requirement over the range (which corresponds to the decrease in solvent circulation rates required to achieve 90% CO₂ capture). Relatively marginal savings could be achieved from 27 m and above. There could be considerable operational savings with higher packing heights that would compensate for the additional capital costs required. For the remaining case studies (in Sections 5.2 to 5.4), 27 m of absorber packing height was used.

5.2. Case study 2 - plant performance with different concentrations of MEA

The whole plant performance with different concentrations of MEA is shown in Table 4 and compared to the base case without CO₂ capture. As discussed in Section 3.2, the fuel burn rate in the power plant is manipulated to control the drum pressure. The set point of the drum pressure is set to achieve a certain power output. In all cases presented in Table 4, the target power output was set to

500 MWe. However, due to the amount of steam drawn off for regeneration in the CO₂ capture cases, it was impossible to achieve the target and the actual or net power plant output depended on the amount of steam drawn off.

Power plant efficiency, η , is calculated as follows:

$$\eta = \frac{\text{net power output}}{\text{fuel burn rate} \times \text{NCV}} \quad (21)$$

The net power output was estimated by accounting for the power consumption of the various auxiliaries (estimated as 15 MWe). This net power output corresponds to the electrical power generated.

With carbon capture, the power plant efficiency drops from 37.2% to the values given in Table 4 (it should be noted that the power requirement for CO₂ product compression is not considered in this study).

In summary, an increase in MEA concentration leads to easier CO₂ capture and less requirement for steam draw-off. The power plant efficiency is seen to increase with MEA concentration. For comparison, the fuel burn rate was set to a constant value of 56.8 kg/s (which produced 500 MWe in the base case without capture) for all three cases. 30 wt.% MEA is typically employed in the chemical absorption process. 20 wt.% concentration would necessitate relatively higher solvent circulation rates which would increase the heat duty demanded by the reboiler to raise the temperature of the solvent circulated to the set point. On the other hand, this configuration required the least amount of pure MEA solvent (about 727 kg/s) and at that concentration, would pose the least challenge in terms of corrosion. MEA concentration (40 wt.%) would require the most solvent (1149 kg/s compared to 912 kg/s at 30 wt.%) and would have the most severe corrosion challenges. With increased MEA concentration, more heat of reaction is released whilst absorbing CO₂ with less solvent circulation. As a result, the absorber temperatures increase as shown in Table 4 and the efficiency of the absorption process thus reduces. Some savings could be achieved if temperatures are lowered in the column through techniques such as inter-cooling especially at higher concentrations of MEA solvent.

5.3. Case study 3 - reducing target power output

This case simulates the effect of a decrease in target power output over a period of 10 min. Power plant target output was ramped down from 440 to 415 MWe over the aforementioned time period. The net power output is determined by the power plant power output controllers which manipulate the fuel burn rate and governor valve opening to meet the target power output. The capture level controller set point was maintained at 90% CO₂ capture. Base case conditions were maintained for 4 h before the disturbance was introduced. The whole plant model was then simulated for another 10 h. Results of the simulation are shown in Figs. 11 and 12.

Fig. 11a shows the drop in net power output with time. The fuel burn rate is adjusted to achieve this drop (Fig. 11b). With a reduced

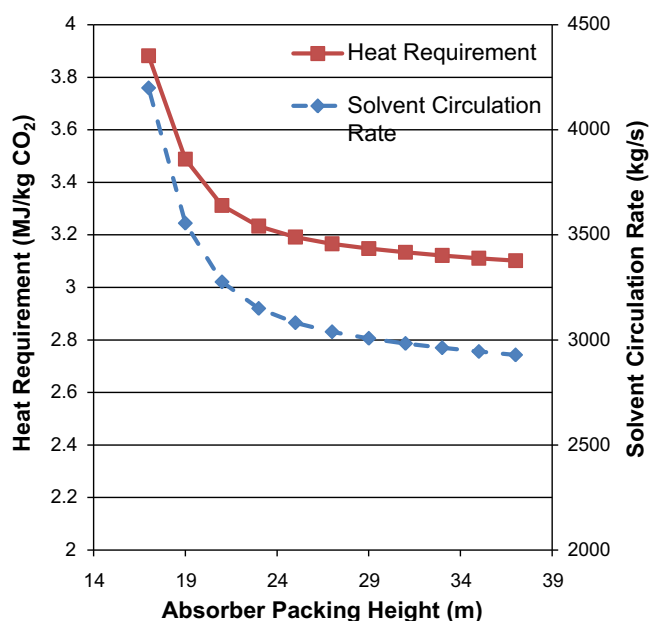


Fig. 10. Plant performance with different absorber packing heights.

Table 4

Summary of parameters for the whole plant model with and without CO₂ capture and at different MEA concentrations.

Description	Without CO ₂ Capture	With CO ₂ capture (20 wt.% MEA)	With CO ₂ capture (30 wt.% MEA)	With CO ₂ capture (40 wt.% MEA)
CO ₂ capture level (%)	0	90	90	90
solvent circulation rate (kg/s)	0	3663	3122	2964
Flue gas flow rate (kg/s)	589.6	589.6	589.6	589.6
Net power output (MWe)	500	437	453	467
Fuel burn rate (kg/s)	56.8	56.8	56.8	56.8
Power plant efficiency	37.2	30.0	31.1	32
Steam draw-off flow rate (% of steam flow rate from IP turbine exit)	0	54	42	34
Maximum absorber temperature (K)	N/A	335	338	340

fuel burn rate, the flue gas produced reduces correspondingly and thus the flow of gas to the absorber column reduces. With less gas to process in the absorber, less solvent circulation is required (Fig. 11d). The heat duty required in the reboiler to regenerate solvent thus decreases correspondingly and there is therefore a reduced demand for steam from the power generation process (Fig. 11c). The power plant efficiency (Fig. 11e) shows some initial perturbations before settling down to roughly the same steady state value. The CO₂ capture level (Fig. 11f) also oscillates and steadies at the controller's set point of 90%.

Fig. 12 shows the same results in terms of their percentage deviation from their original values (before the onset of the disturbance). By close observation, certain features become more apparent. For instance, the solvent circulation rate shows the largest deviation perhaps because its settings provide tight control of the capture level. Again from Fig. 12, the capture level does not vary much. Even as such, there are periods where the capture level is above the set point and more importantly below the set point as well. If emission regulations are such that the capture level must not go below a certain value at any point in time, it is advisable to operate the capture plant sufficiently above the minimum value so that disturbances from the power plant do not drop the capture level below it. From Section 5.4, it is shown that achieving higher capture levels becomes increasingly difficult as 100% capture is approached so care must be taken to select appropriate operating capture levels.

In addition, because of the tight controls on capture level and the resulting oscillations in solvent circulation rates, the power plant power output oscillates in response to changing steam draw-off rates from the IP/LP crossover. From Figs. 11a and 12, the power plant output drops below the set point and takes a while to settle at the set point making it difficult to achieve steady power output levels quickly. In this case, it appears that the tight control on capture level is interfering with the power plant power output control.

The response of the power plant to operational changes is relatively fast. From the onset of the disturbance (reducing the power plant output) the change in fuel burn rate and subsequently flue gas flow rate is relatively fast. In addition, the capture level and solvent circulation rates also change soon after this disturbance is introduced. However, the response of the amine plant is much slower. For instance, with a reduction in the solvent circulation rate, a lower heat duty is demanded in the reboiler. However, from Fig. 12, there is clearly a delay in the response of the steam draw-off rate compared with that of the solvent circulation rate. This shows that the process dynamics of CO₂ capture plant is relatively slow compared to that of the power plant. The manipulation of solvent circulation rate (and subsequently steam draw-off rate) in turn imposes some disturbances on the power generation process. It is therefore, not advisable to have such tight control on the capture level considering the interaction of this control loop with the power plant power output control.

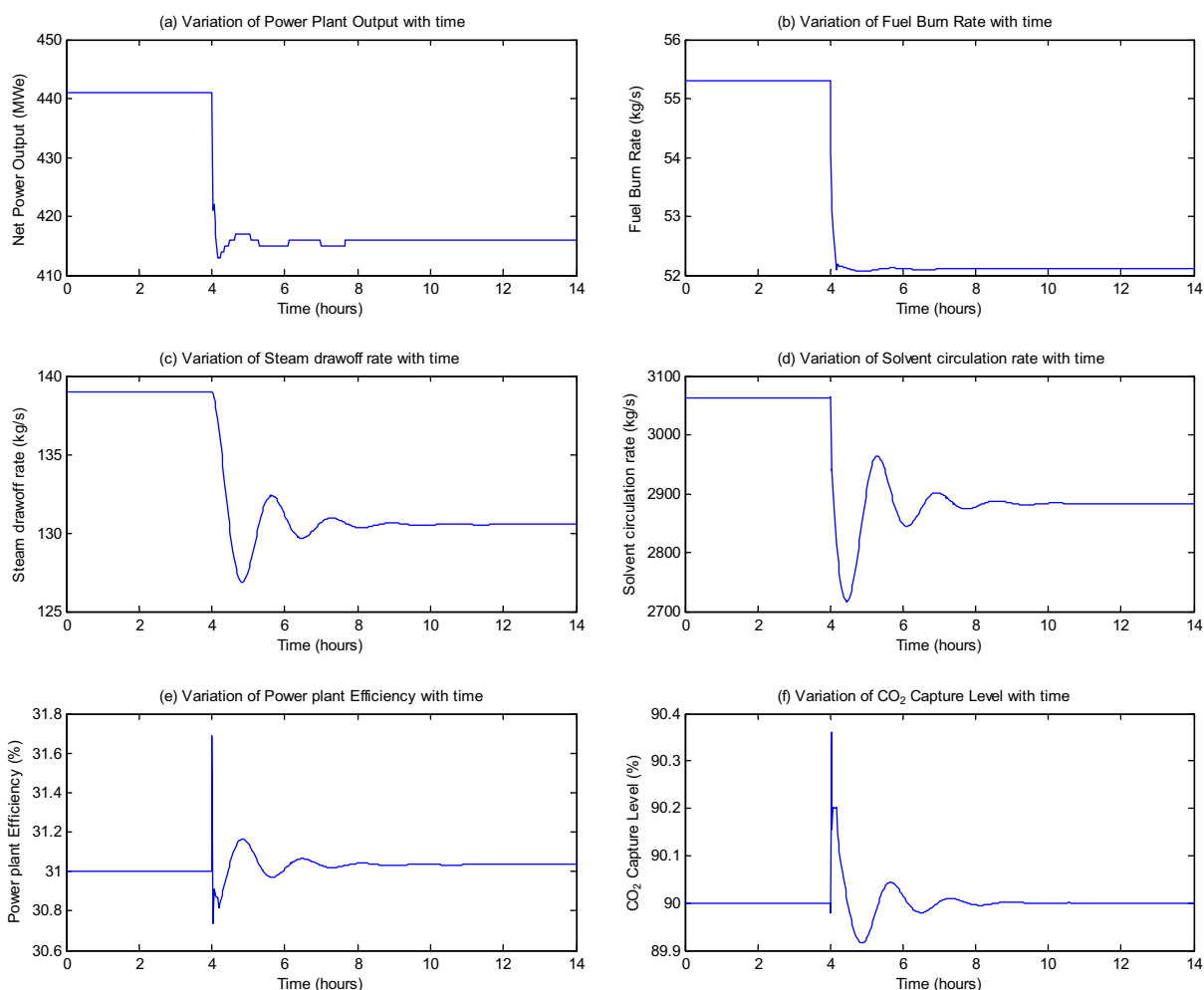


Fig. 11. Effects of decreasing target power plant output.

5.4. Case study 4 – increasing CO₂ capture level set point to 95%

This case simulates the change in CO₂ capture level set point in the capture level controller from the base case value of 90% to 95%.

Power output targets were maintained. Base case conditions were maintained for 4 h before the disturbance was introduced. The whole plant model was then simulated for another 10 h. Results of the simulation are shown in Figs. 13 and 14.

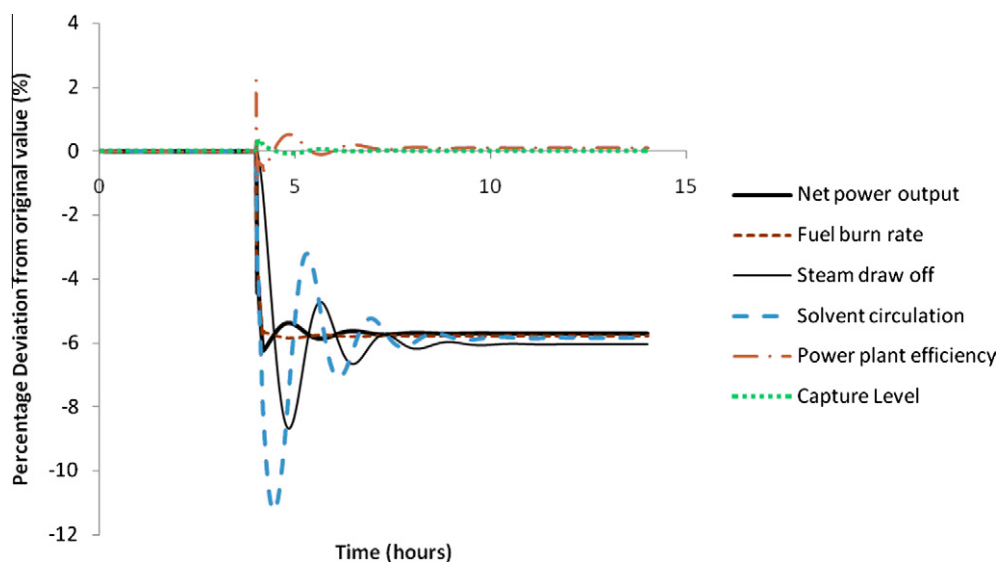


Fig. 12. Percentage deviations with decreasing target power plant output.

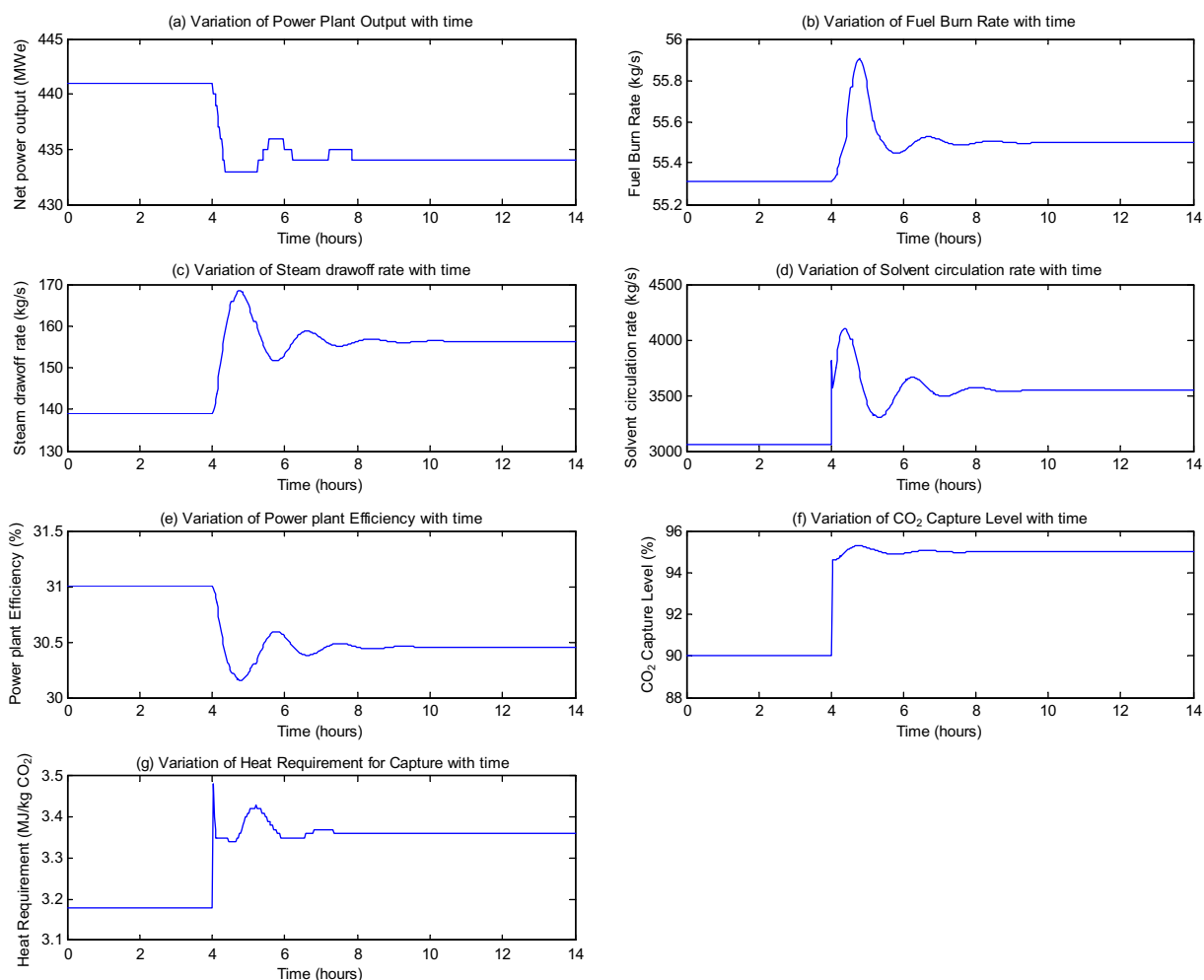


Fig. 13. Effects of Increasing CO₂ capture level set point.

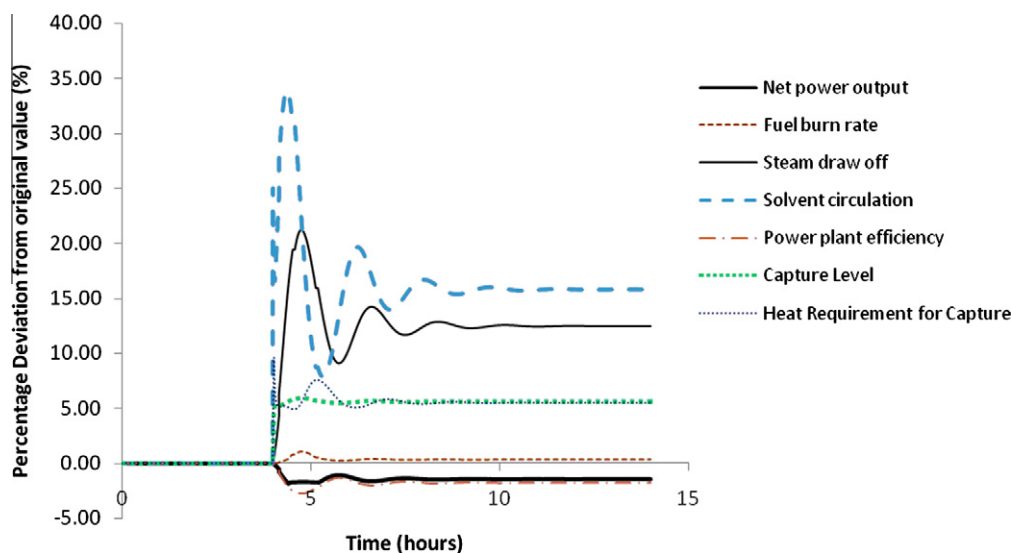


Fig. 14. Percentage deviations with increasing CO₂ capture level set point.

Fig. 13a shows the power plant power output changes with time. Roughly, a 1.8% reduction in power plant output is observed after the disturbance (Fig. 14). The fuel burn rate increases to compensate for the loss in power output (Fig. 13b). It then steadies at a slightly higher value than before the disturbance. Increasing the capture level set point would imply increased solvent circulation rates (Fig. 13d). This increase attains a maximum of 34% (Fig. 14) before it steadies at almost 16% although the CO₂ capture level was increased by only 5% points (Fig. 13f). This confirms that as 100% capture level is approached, CO₂ capture becomes increasingly difficult. This is clearly seen from Fig. 13g where there is an increase in heat requirement for CO₂ capture after the disturbance was introduced. This value measures how much heat is required to separate 1 kg of CO₂. It increases by just over 5% and appears to correspond to the increase in capture level at steady state (Fig. 14).

The power plant efficiency reduces by almost 2.5% before attaining a steady state value 1.7% less than original due to the disturbance (Figs. 13e and 14). From observing Fig. 13c and e, it could be concluded that the efficiency reduction follows the response of the steam draw-off.

Both dynamic case studies show possible negative effects a poor control system or strategy could have on the integrated operation of a post-combustion capture plant. Better process control could be achieved with improved controller tuning.

6. Conclusions

Dynamic models of the power plant and CO₂ capture plant have been developed, validated and linked. The scale-up of the CO₂ capture plant from pilot plant scale (where it was validated) to the scale required for processing flue gas from a 500 MWe sub-critical power plant was described. Four case studies were considered. The first investigates the whole plant performance with and without CO₂ capture. For the cases with CO₂ capture, 20, 30 and 40 wt.% MEA solution was utilized. The power plant efficiency was highest with the 40 wt.% case as expected and further improvements may be possible with the application of techniques such as inter-cooling. At such high solvent concentrations, more quantities of corrosion inhibitors would be required. From the investigations carried out, selecting 27 m of absorber packing height offered a good balance between increasing column costs and reducing heat requirement in the reboiler. The two dynamic case studies showed that

the CO₂ capture plant has a slower response than the power plant. Dynamic case studies reveal interaction of CO₂ capture level and power plant output control loops. As the CO₂ capture level set point was increased from 90% to 95%, the thermal efficiency of the capture process reduced.

Acknowledgements

This work is partly funded by RWE npower and its support is greatly appreciated. The technical support from Process Systems Enterprise (PSE) Ltd, UK is also appreciated. The authors at Cranfield University would also like to acknowledge the financial support from Research Council UK Energy Programme (Ref: NE/H013865/1).

References

- [1] Okuzumi N, Mitchell R. Current status of MHI's CO₂ recovery technology and road map to commercialization for coal fired power plant application. In: International conference and exhibition: nitrogen and syngas. Bahrain, March 2010. <www.mhi.co.jp/en/products/pdf/articles_07.pdf>.
- [2] BERR. Advanced power plant using high efficiency boiler/turbine. Report BPB010. BERR, Department for Business Enterprise and Regulatory Reform; 2006. <www.berr.gov.uk/files/file30703.pdf>.
- [3] Abu-Zahra MRM, Schneiders LHJ, Niederer JPM, Feron PHM, Versteeg GF. CO₂ capture from power plants: Part I. A parametric study of the technical performance based on monoethanolamine. Int J Greenhouse Gas Control 2007;1(1):37–46.
- [4] Davidson R. Post-combustion carbon capture from coal fired plants – solvent scrubbing. Report CCC/125. IEA Clean Coal Centre; 2007. <www.iea-coal.org.uk>.
- [5] Davison J. Performance and costs of power plants with capture and storage of CO₂. Energy 2007;32(7):1163–76.
- [6] Herzog H, Meldon J, Hutton A. Advanced post-combustion CO₂ capture; 2009. <web.mit.edu/mitei/docs/reports/herzog-meldon-hutton.pdf>.
- [7] Kvamsdal HM, Jakobsen JP, Hoff KA. Dynamic modelling and simulation of a CO₂ absorber column for post-combustion CO₂ capture. Chem Eng Process: Process Intensification 2009;48(1):135–44.
- [8] Lawal A, Wang M, Stephenson P, Yeung H. Dynamic modelling of CO₂ absorption for post-combustion capture in coal-fired power plants. Fuel 2009;88(12):2455–62.
- [9] Ziaii S, Rochelle GT, Edgar TF. Dynamic modeling to minimize energy use for CO₂ capture in power plants by aqueous monoethanolamine. Ind Eng Chem Res 2009;48(13):6105–11.
- [10] Lawal A, Wang M, Stephenson P, Yeung H. Dynamic modeling and simulation of CO₂ chemical absorption process for coal-fired power plants. Comput Aided Chem Eng 2009;27:1725–30.
- [11] Lawal A, Wang M, Stephenson P, Koumpouras G, Yeung H. Dynamic modelling and analysis of post-combustion CO₂ chemical absorption process for coal-fired power plants. Fuel 2010;89(10):2791–801.

- [12] Lawal A, Wang M, Stephenson P. Investigating the dynamic response of CO₂ chemical absorption process in enhanced-O₂ coal power plant with post-combustion CO₂ capture. vol. 3. Energy Procedia; 2010.
- [13] Lu S. Dynamic modelling and simulation of power plant systems. Proc IMechE Part A 1999;213:7–22.
- [14] Åström KJ, Bell RD. Drum boiler dynamics. Automatica 1999;36:363–78.
- [15] Bhambare KS, Sushanta KM, Gaitonde UN. Modelling of coal fired natural circulation boiler. Trans ASME 2009;129:159–66.
- [16] Chaibakhsh A, Ghaffari A, Moosavian SAA. A simulated model for a once-through boiler by parameter adjustment based on genetic algorithms. Simulat Model Pract Theory 2007;15(9):1029–51.
- [17] Stephenson P, Tian J, Jovanovic S, Tian X. Steady-state and dynamic modelling for a hybrid approach to post-combustion capture of carbon dioxide. In: Proceedings of the 12th IEA GHG post-combustion international networking meeting. Canada: University of Regina; September 2009.
- [18] Aroonwilas A, Veawab A. Integration of CO₂ capture unit using single- and blended-amines into supercritical coal-fired power plants: Implications for emission and energy management. Int J Greenhouse Gas Control 2007;1: 143–50.
- [19] Sanpasertparnich T, Idem R, Bolea I, deMontigny D, Tontiwachwuthikul P. Integration of post-combustion capture and storage into a pulverised coal-fired power plant. Int J Greenhouse Gas Control 2010;4(3):499–510.
- [20] Cifre PG, Brechtel K, Hoch S, Garcia H, Asprion N, Hasse H, et al. Integration of a chemical process model in a power plant modelling tool for the simulation of an amine based CO₂ scrubber. Fuel 2009;88(12):2481–8.
- [21] Dugas ER. Pilot plant study of carbon dioxide capture by aqueous monoethanolamine, M.S.E. Thesis, University of Texas at Austin; 2006.
- [22] Oyenakan BA. Modeling of strippers for CO₂ capture by aqueous amines. University of Texas at Austin; 2007.
- [23] Ramezan M, Skone TJ. Carbon dioxide capture from existing coal-fired power plants. Report DOE/NETL-401/110907, National Energy Technology Laboratory (NETL); 2007.
- [24] Sinnott RK. Chemical engineering design. 4th ed. Oxford, UK: Butterworth-Heinemann; 2005.
- [25] Stichlmair JG, Fair JR. Distillation: principles and practices. New York: Wiley-VCH; 1998.
- [26] Sidders JA. ANYDYM – a fossil fired total plant model, Report PKR/SE/255; 1989.
- [27] Lucquiaud M, Gibbins J. Retrofitting CO₂ capture ready fossil plants with post-combustion capture. Part 1: requirements for supercritical pulverized coal plants using solvent-based flue gas scrubbing. In: Proceedings of the Institution of Mechanical Engineers, Part A: Journal of Power and Energy 2009; 223(3):2041–967.
- [28] Cooke DH. On prediction of off-design multistage turbine pressures by Stodola's Ellipse. J Eng Gas Turb Power 1985;107(3):596–606.